Original Article
J Vet Sci 2018, 19(2), 216-231 · https://doi.org/10.4142/jvs.2018.19.2.216

JVS

Analysis of protein expression in *Brucella abortus* mutants with different growth rates by two-dimensional gel electrophoresis and LC-MS/MS peptide analysis

Woo Bin Park[1], Young Bin Im[1], Soojin Shim[1], Han Sang Yoo[1,2,*]

[1]*Department of Infectious Diseases, College of Veterinary Medicine, Seoul National University, Seoul 08826, Korea*
[2]*Institute of Green-Bio Science and Technology, Seoul National University, Pyeongchang 25354, Korea*

Brucella abortus is a bacterium that causes brucellosis and is the causative agent of worldwide zoonoses. Pathogenesis of the *B. abortus* infection is complicated, and several researchers have attempted to elucidate the infection mechanism of *B. abortus*. While several proteins have been revealed as pathogenic factors by previous researchers, the underlying mechanism of *B. abortus* infection is unresolved. In this study, we identified proteins showing different expression levels in *B. abortus* mutants with different biological characteristics that were generated by random insertion of a transposon. Five mutants were selected based on biological characteristics, in particular, their growth features. Total proteins of mutant and wild-type *B. abortus* were purified and subjected to two-dimensional gel electrophoresis. Thirty protein spots of each mutant with expression increases or decreases were selected; those with a change of more than 2-fold were compared with the wild-type. Selected spots underwent liquid chromatography tandem mass spectrometry for peptide analysis. DnaK and ClpB, involved in protein aggregation, increased. SecA and GAPDH, associated with energy metabolism, decreased in some mutants with a growth rate slower than that of the wild-type. Mutants with slower growth showed a decrease in energy metabolism-related proteins, while mutants with faster growth showed an increase in pathogenicity-related proteins.

Keywords: *Brucella abortus*, growth rates, protein sequence analysis, two-dimensional gel electrophoresis

Introduction

Brucella abortus is a bacterium that cause brucellosis and is the causative agent of a worldwide zoonotic disease that infects both humans and animals. Brucellosis generally causes persistent abortion and infertility in infected animals and can cause serious economic damage. In the case of human infection, symptoms include undulant fever and arthritis [3,11]. *B. abortus* has a small, non-motile, non-spore forming bacterium with a rod shape. Due to the survival characteristics of bacteria at the intracellular level, they are very difficult to isolate. Unlike other pathogenic bacteria, *B. abortus* does not produce exotoxins, toxic lipopolysaccharide, fimbriae, or plasmids [10]. *B. abortus* is a Gram-negative facultative intracellular pathogen that can enter to the host macrophage and survive. Due to its intracellular survival characteristics, its isolation is complicated. *B. abortus* does not utilize the classical pathogenicity factors mentioned above; rather, it invades and proliferates in host phagocytic cells, thereby avoiding the host's cell-mediated immune reaction. This infection mechanism allows it to survive for a long time in the host and can result in chronic infection [21].

Intracellular pathogens are commonly exposed to a variety of environmental factors, including stresses such as pH, oxidation, and nutrition. The survival of *B. abortus* in macrophages is closely related to the production of various proteins. For example, in the case of heat-shock protein, produced when cells are exposed to high temperatures or other stresses, intracellular bacteria can adapt to a stressful environment [30]. In addition, Hfq, an RNA-binding protein, also has a role in adapting to various stressful environments. It has been reported that, when *hfq* mutation occurs, several genes associated with the cellular processes are not properly regulated [7]. Several attempts have been made to solve the mechanism of *Brucella* infection [8,21]. Although several proteins have been proposed as potentially pathogenic, the basic mechanism of *B. abortus* infection still

Received 18 May 2017, Revised 12 Sep. 2017, Accepted 22 Sep. 2017
*Corresponding author: Tel: +82-2-880-1263; Fax: +82-2-874-2738; E-mail: yoohs@snu.ac.kr
pISSN 1229-845X
eISSN 1976-555X

needs to be described [21].

Post-genomic technology provides a new and exciting opportunity for further research into and understanding of *B. abortus* [13]. Various studies on the immunogenic components of *B. abortus* can be conducted based on proteomic studies for the detection of various antigens [14]. The post-genome approach of proteomics using two-dimensional gel electrophoresis (2-DE) can be used to discover, isolate, and identify new antigens that are different from previously reported ones [14,22,29].

Five mutants were selected for study after analyzing the molecular characteristics of *B. abortus* wild-type and several mutants [20]. The purpose of this study was to investigate protein expression levels of the selected *B. abortus* mutants. In

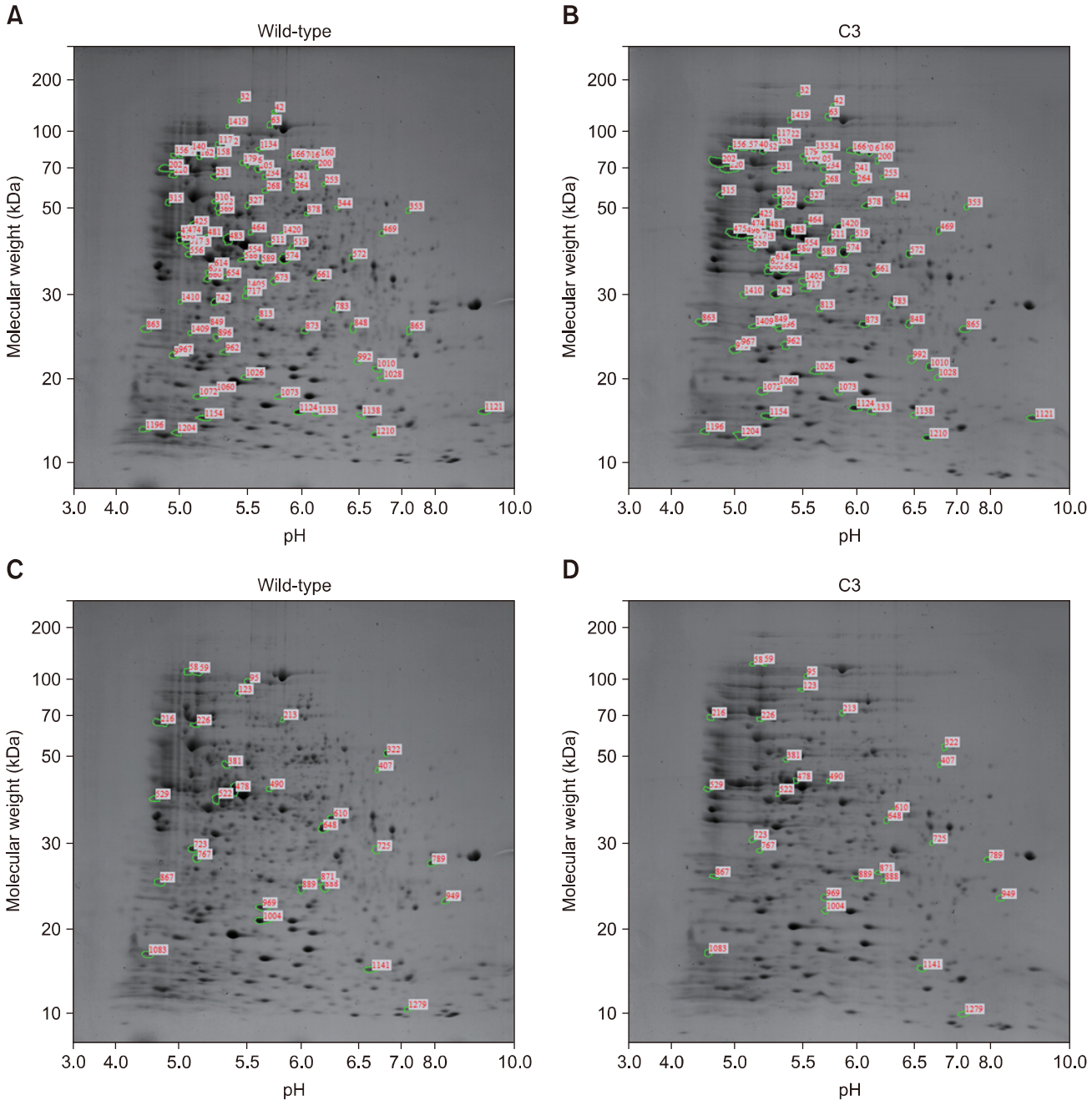

Fig. 1. Two-dimensional gel electrophoresis (2-DE) image analysis of *Brucella abortus* wild-type and *B. abortus* mutant C3. (A) 2-DE image of *B. abortus* wild-type. (B) 2-DE image of *B. abortus* mutant C3. (C) Spots of *B. abortus* mutant C3 that were relatively increased compared to *B. abortus* wild-type. (D) Spots of *B. abortus* mutant C3 that were relatively decreased compared to *B. abortus* wild-type.

addition, we examined the relationships between protein expression level changes and the growth features of *B. abortus* mutants.

Materials and Methods

Sample selection and preparation for 2-DE

B. abortus mutants were prepared by transposon mutagenesis using wild-type and kanamycin resistance (*rKan*) genes and the EZ-Tn5 transposon system (Epicentre Biotechnologies, USA). The mutants were used in experiments to assess changes in

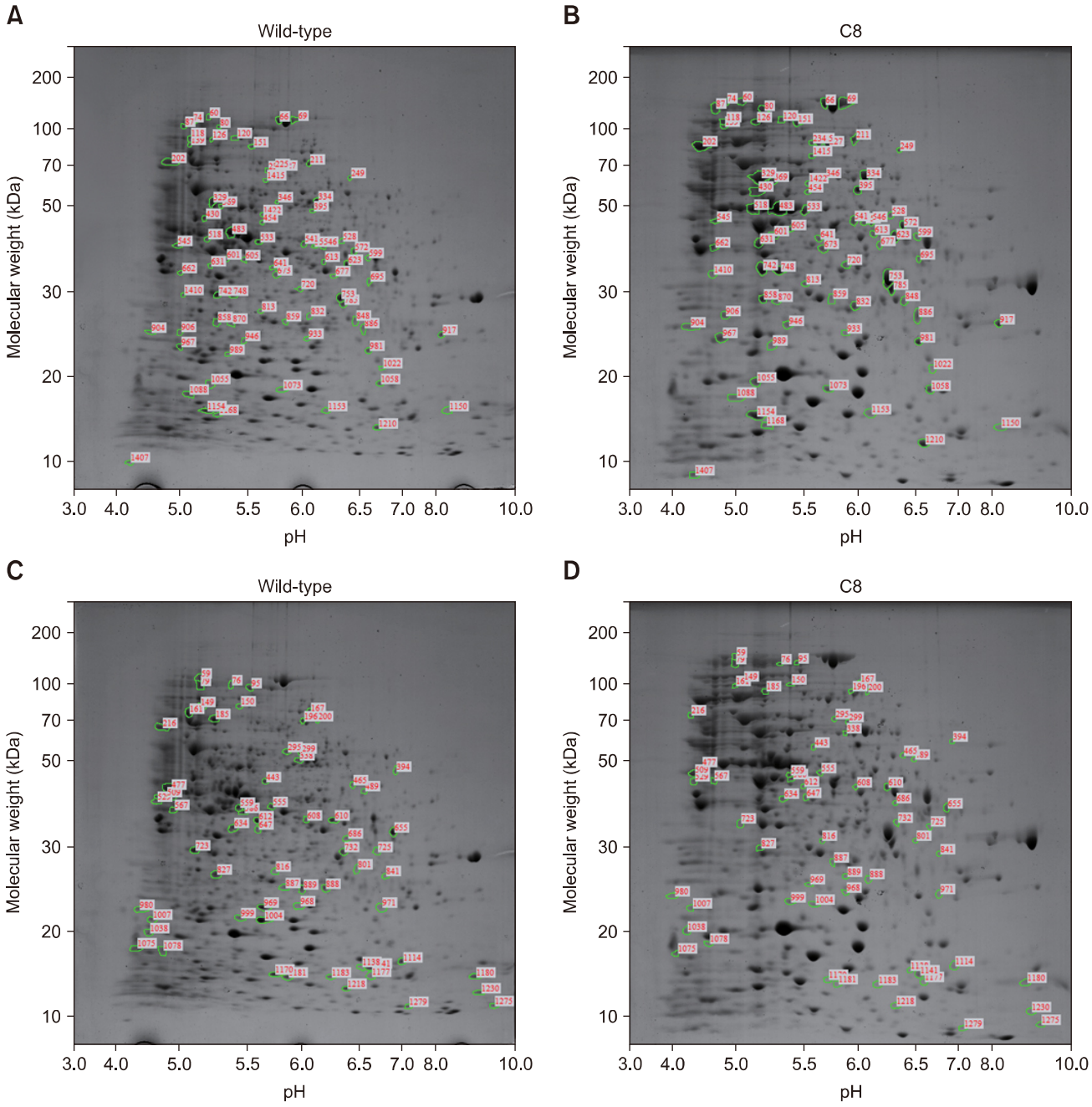

Fig. 2. Two-dimensional gel electrophoresis (2-DE) image analysis of *Brucella abortus* wild-type and mutant C8. (A) 2-DE image of *B. abortus* wild-type. (B) 2-DE image of *B. abortus* mutant C8. (C) Spots of *B. abortus* mutant C8 that were relatively increased compared to *B. abortus* wild-type. (D) Spots of *B. abortus* mutant C8 that were relatively decreased compared to *B. abortus* wild-type.

characteristics such as growth feature and pathogenic factors following *rKan* insertion. Biochemical tests were performed on *B. abortus* wild-type and 24 *B. abortus* mutants. Five mutants were selected based on growth features [20]. The selected *B. abortus* mutants C3, C8, and C13 had a slower growth pattern than *B. abortus* wild-type, whereas selected *B. abortus* mutants C24 and C30 had a faster growth pattern than *B. abortus* wild-type.

B. abortus wild-type cultured in 10 mL Brucella broth (BD, USA) for 24 h was used as a seed in 250 mL Brucella broth (BD) for 24 h. *B. abortus* mutants C3, C8, C13, C24, and C30 from 10 mL cultures grown in Brucella broth (BD) with kanamycin (100 µL/500 mL; Sigma, USA) for 24 h were used as seeds in 250 mL Brucella broth (BD) with kanamycin (100 µL/500 mL; Sigma)

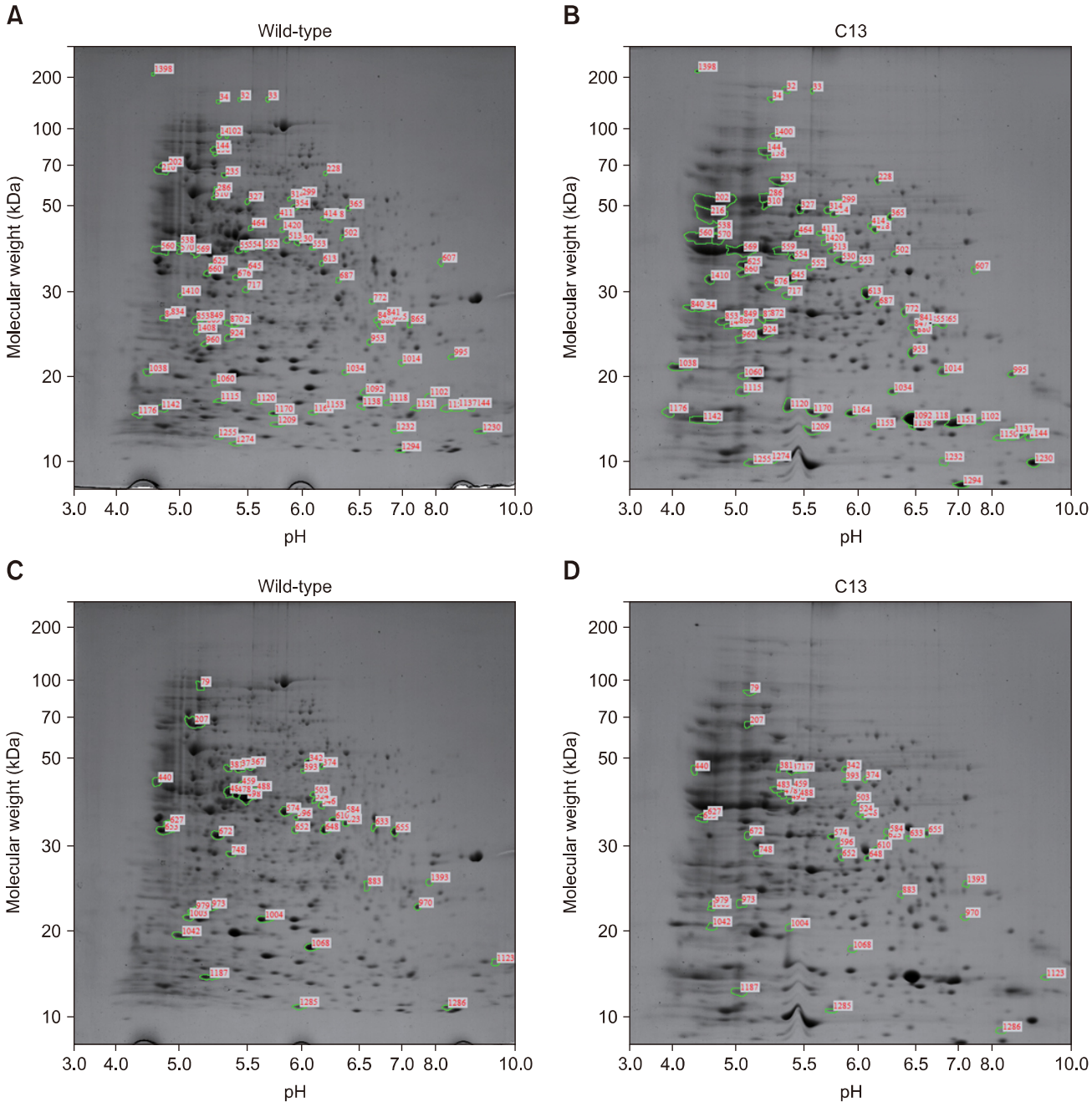

Fig. 3. Two-dimensional gel electrophoresis (2-DE) image analysis of *Brucella abortus* wild-type and mutant C13. (A) 2-DE image of *B. abortus* wild-type. (B) 2-DE image of *B. abortus* mutant C13. (C) Spots of *B. abortus* mutant C13 that were relatively increased compared to *B. abortus* wild-type. (D) Spots of *B. abortus* mutant C13 that were relatively decreased compared to *B. abortus* wild-type.

for 24 h. These were harvested via centrifugation at 8,000 × g for 30 min at 4°C. The pellets were washed twice with PBS. All procedures were approved by the Seoul National University Institutional Biosafety Committee (SNUIBC-R160314-1).

2-DE analysis

The 2-DE was carried out essentially as described. *B. abortus* wild-type and 5 mutants in sample buffer (7 M urea, 2 M thiourea, 4.5% CHAPS, 100 mM DTE, 40 mM Tris, pH 8.8) were applied to immobilized pH 3 to 10 nonlinear gradient strips (Amersham Biosciences, Sweden) for isoelectric focus (IEF). Similar amounts of each protein from *B. abortus* wild-type and mutants underwent 2-DE analysis after quantification. IEF was performed at 80,000 Vh. The second

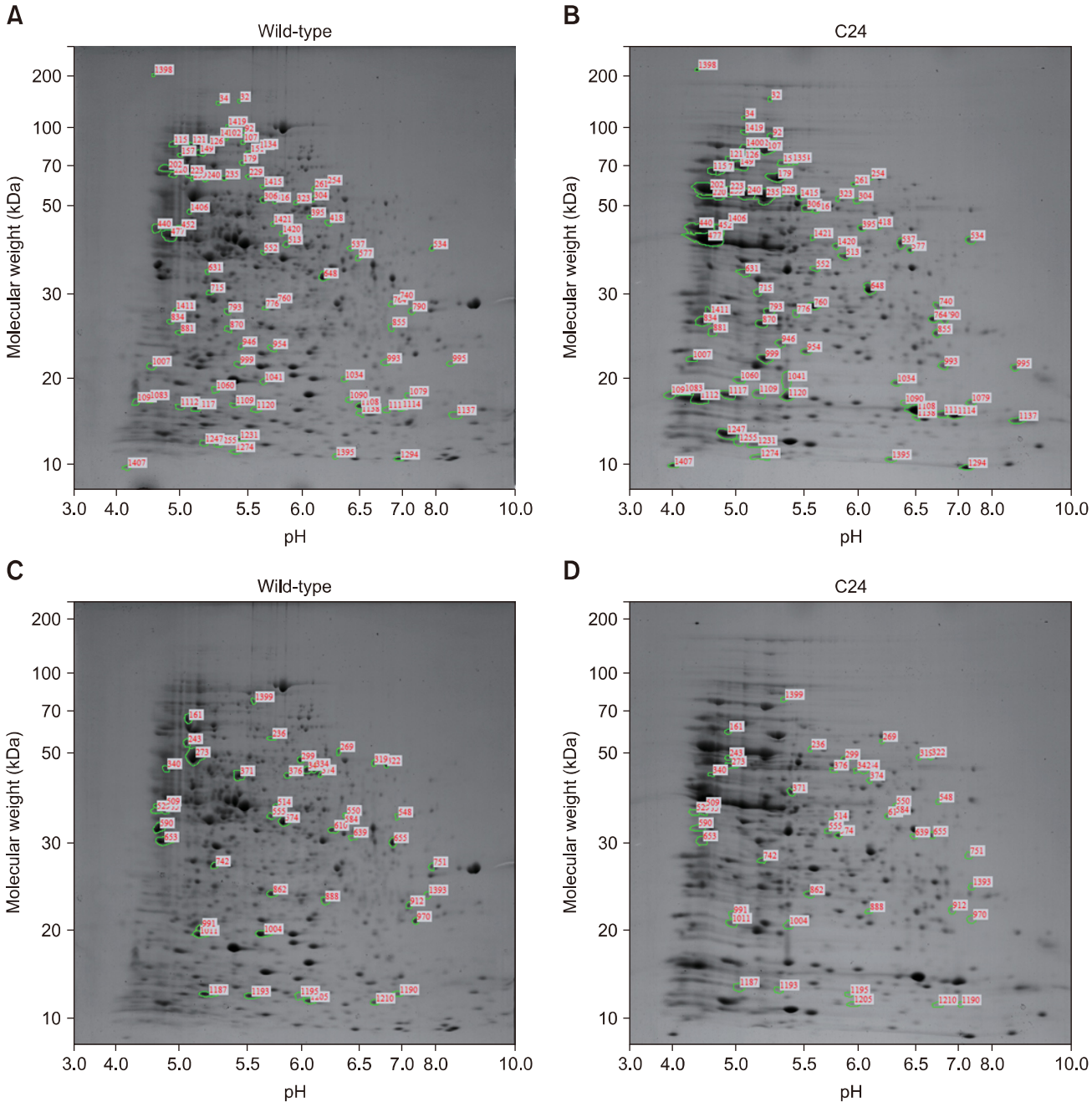

Fig. 4. Two-dimensional gel electrophoresis (2-DE) image analysis of *Brucella abortus* wild-type and mutant C24. (A) 2-DE image of *B. abortus* wild-type. (B) 2-DE image of *B. abortus* mutant C24. (C) Spots of *B. abortus* mutant C24 that were relatively increased compared to *B. abortus* wild-type. (D) Spots of *B. abortus* mutant C24 that were relatively decreased compared to *B. abortus* wild-type.

dimension was analyzed on 9% to 16% linear gradient polyacrylamide gels (18 cm × 20 cm × 1.5 cm) at constant 40 mA per gel for approximately 5 h. After protein fixation in 40% methanol and 5% phosphoric acid for 1 h, the gels were stained with Coomassie brilliant blue G-250 for 12 h. The gels were then destained with distilled water, scanned in a Bio-Rad GS710 densitometer (Bio-Rad, USA) and converted to electronic files, which were then analyzed by using the Image Master Platinum 5.0 image analysis program (Amersham Biosciences) [16,17].

Liquid chromatography tandem mass spectrometry (LC-MS/MS) for peptide analysis

According to the results of 2-DE analysis, we selected 30

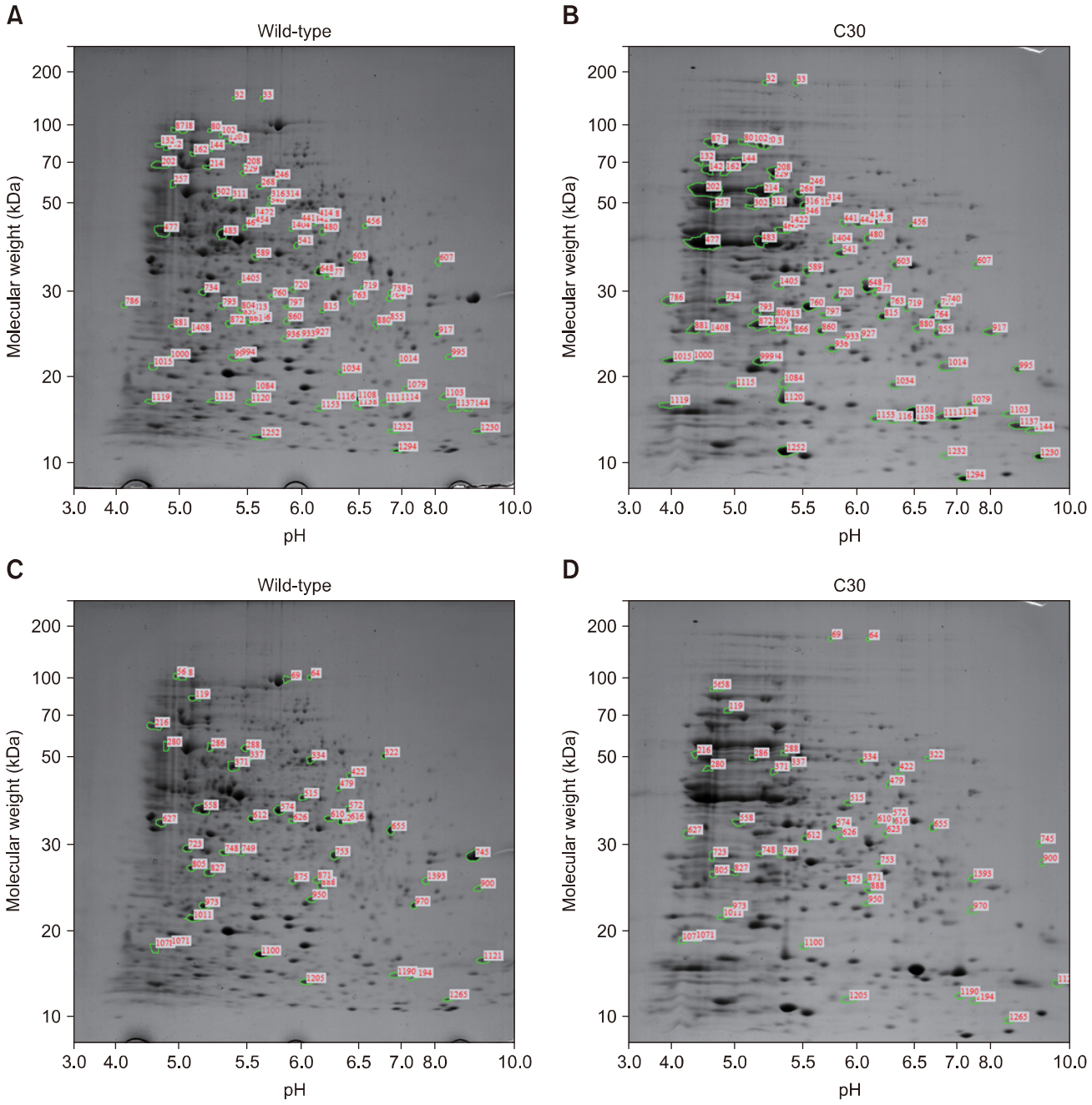

Fig. 5. Two-dimensional gel electrophoresis (2-DE) image analysis of *Brucella abortus* wild-type and mutant C30. (A) 2-DE image of *B. abortus* wild-type. (B) 2-DE image of *B. abortus* mutant C30. (C) Spots of *B. abortus* mutant C30 that were relatively increased compared to *B. abortus* wild-type. (D) Spots of *B. abortus* mutant C30 that were relatively decreased compared to *B. abortus* wild-type.

spots from each image of the *B. abortus* mutants that had higher than 2-fold changes (increase or decrease) from those of *B. abortus* wild-type. LC-MS/MS for peptide analysis was performed on the selected spots.

Nano LC-MS/MS analysis was performed with an Easy n-LC chromatograph (Thermo Fisher, USA) and a LTQ Orbitrap XL mass spectrometer (Thermo Fisher) equipped with a nano-electrospray source. Protein samples were separated on a C18 nano bore column (150 mm × 0.1 mm, 3 μm pore size; Agilent, USA). Mobile phase A for LC separation was 0.1% formic acid, 3% acetonitrile in deionized water, while mobile phase B was 0.1% formic acid in acetonitrile. The chromatography gradient was designed for a linear increase from 5% B to 30% B in 23 min, 30% B to 60% B in 3 min, 95% B in 3 min, and 3% B in 6 min. The flow rate was maintained at 1,500 nL/min. Mass spectra were acquired by using data-dependent acquisition with a full mass scan (350−1,200 m/z) followed by 10 MS/MS scans. For MS 1 full scans, the orbitrap resolution was 15,000 and the AGC was 2×10^5. For MS/MS in the LTQ, the AGC was 1×10^4 [15].

Database searching

Analysis and interpretation of the LC-MS/MS data were conducted according to the Mascot algorithm (Matrix Science, USA), which was used to identify peptide sequences present in a protein sequence database. Database search criteria were: taxonomy, *B. abortus* bv. 1 str. 9-941 (downloaded 12 April 2016; National Center for Biotechnology Information, USA); fixed modification; carbamidomethylated at cysteine residues; variable modification; oxidized at methionine residues; maximum allowed missed cleavage, 2; MS tolerance, 10 ppm; MS/MS tolerance, 0.8 Da. The peptides were filtered with a significance threshold of $p < 0.05$.

Results

For this study, five mutants, among 24 mutants showing differences in growth features from those of *B. abortus* wild-type [20], were selected. The mutants were commonly resistant to kanamycin and were expected to show differences in protein expression following insertion of the *rKan* gene.

The 2-DE analysis, using the same concentrations of prepared proteins from *B. abortus* wild and mutant strains, revealed 814 spots in *B. abortus* wild-type and 541 spots in mutant C3. Among them, 444 paired spots were identified after comparison of the mutants with *B. abortus* wild-type. Ninety-four spots showed increases and 30 showed decreases from *B. abortus* wild-type (Fig. 1). In case of mutant C8, the total number of spots was 577, and 418 spots were paired with *B. abortus* wild-type. Among them, 78 spots showed relatively increased expression and 65 spots showed decreased expression (Fig. 2). In mutant C13, the total number of spots were 491, of which 256 spots formed pairs with *B. abortus* wild-type. Among them, 87 spots were relatively increased and 43 spots were decreased (Fig. 3). The total spot number of mutant C24 was 516, of which 246 spots formed pairs with *B. abortus* wild-type. Of these, 87 spots increased in relative expression and 45 spots had decreased expression (Fig. 4). A total of 560 spots were identified in mutant C30, of which 282 spots formed pairs with *B. abortus* wild-type. In 96 spots of those spots, expression was relatively increased, while in 50 spots, expression was decreased (Fig. 5, Table 1). All spots were detected on 2-DE gels and had *pI* (isoelectric point) and molecular weight ranges of 4.0 to 10.0 and 10 to 250 kDa, respectively. Based on the 2-DE image analysis results, 30 spots of each mutant strain with greater than 2-fold changes (increases or decreases) from those of the spots of *B. abortus* wild-type were selected. The selected spots underwent LC-MS/MS for peptide analysis (Table 2). The spot number, gene name, gene ID, protein identification, protein ID, accession number, sequence length, locus tag, experimental molecular weight, theoretical molecular weight, *pI*, sequence coverage (%), subcellular location, and Clusters of Orthologous Groups (COG) functional category of these proteins are presented in Table 3.

Table 1. Two-dimensional electrophoresis results for *Brucella abortus* wild-type and *B. abortus* mutants

Group	Spots	Paired spots	Spots increased more than 2-fold	Spots decreased more than 2-fold
Wild-type Reference	814	–	–	–
C3	541	444	93	30
C8	577	418	78	65
C13	491	256	87	43
C24	516	246	87	45
C30	560	282	96	50

The results confirmed that expressions of pathogenic factors such as ClpB and its interacting DnaK, RpsE, and cold-shock proteins were increased; particularly in mutants C24 and C30. In some mutants, an increase in proteins related to energy metabolism such as Zwf, TrpA, and Pgk were identified, and an increase in proteins associated with ATP-binding protein or ABC transporter were also detected.

The SecA, GAPDH, and GNAT family have been shown to reduce expression in energy metabolism-related factors. In particular, expressions of mutants C3 and C8, which have a slower growth rate than that of *B. abortus* wild-type, were observed to decrease in common. Additionally, in mutants C3 and C8, expression of AcnA, which is involved in bacterial growth, was present but was decreased. Expression of Hfq, which is related to stress resistance and pathogenicity, metabolism, and also important in intracellular survival in *B.*

Table 2. Results of two-dimensional gel electrophoresis and liquid chromatography tandem mass spectrometry for peptide analysis revealed the protein name and the increased and decreased fold changes of 30 selected spots

Spot ID	Protein name	C3	C8	C13	C24	C30
Increased spots						
32	MULTISPECIES: sarcosine oxidase subunit alpha [Brucella]	2.3		5.8	3.6	5
102	ClpB, ATP-dependent Clp protease, ATP-binding subunit ClpB			2.2	2.6	3.9
202	chaperone protein DnaK	5.5	2.7	7.6	6.2	7
234	magnesium ion-transporting ATPase, E1-E2 family	2.8	2.3			
369	Zwf, glucose-6-phosphate 1-dehydrogenase	2.4	3.4			
418	DadA, D-alanine dehydrogenase, small subunit			2.8	2.9	2.6
464	carboxyl-terminal protease	2.4		2.9		3.7
483	hypothetical peptide ABC transporter, permease protein	2.3	4.3			2.6
572	hypothetical protein BruAb1_0662	2.9	2.3			
631	methionine-gamma-lyase, hypothetical		2.3	15.9		
673	ArgF, ornithine carbamoyltransferase	2	2.1			
742	ABC transporter, ATP-binding protein	2.1	2.1			
813	TrpA, tryptophan synthase, alpha subunit	3.4	2.8			6.2
848	RpsC, ribosomal protein S3	2.3	2			
855	RpsC, ribosomal protein S3			4.2	2.7	2.7
870	RpsC, ribosomal protein S3		2.6	2.2	10.7	
995	AtpH, ATP synthase F1, delta subunit			4.6	3.6	4.7
1034	single-stranded DNA-binding protein family			4.5	3.2	4.2
1037	RpsE, ribosomal protein S5			6.7	2.9	4
1060	TPR domain protein	2.4		2.2	4.2	
1073	RplM, ribosomal protein L13	2	2.3			
1118	Dut, deoxyuridine 5-triphosphate nucleotidohydrolase			5.3	5.2	5.4
1120	RecName: Full=Outer membrane lipoprotein Omp16			7.6	7.6	9.7
1138	AhpD, alkyl hydroperoxide reductase D	2		3.6	2.2	3.4
1153	conserved hypothetical protein		3	2.9		2.7
1154	sugar-phosphate isomerases, RpiB/LacA/LacB family	2.7	3.9			
1210	RplX, ribosomal protein L24	2.4	2.6			
1294	cold-shock family protein			3.1	2.1	2.3
1410	RpsB, ribosomal protein S2	2.2	3	10		
1420	Pgk, phosphoglycerate kinase	17.7		2	3.9	
Decreased spots						
59	SecA, preprotein translocase, SecA subunit	2.5	2.2			
95	AcnA, aconitate hydratase 1	2.9	9.7			
161	EtfA, electron transfer flavoprotein, alpha subunit		10.4		2.5	
216	MusA, N utilization substance protein A	6.5	10.2			5.5
299	cytosol aminopeptidase family protein		4.9		2.5	
322	RplK, ribosomal protein L11	4.5			4.9	2.9
342	cytosol aminopeptidase family protein			2.1	10.7	
371	MULTISPECIES: glycerol kinase			2.3	2.9	6.1
478	FabB, 3-oxoacyl-(acyl-carrier-protein) synthase I	3.9		4.9		
529	Tuf-1, translation elongation factor Tu	2.5	2.1		2.4	
574	acetylornithine aminotransferase, hypothetical			3	4.3	3.3
610	Gap, glyceraldehyde 3-phosphate dehydrogenase	2.6	2.2	2.6	7.2	12.2
612	renal dipeptidase family protein		14.7			2
648	IlvC, ketol-acid reductoisomerase	7.7		4.1		
653	conserved hypothetical protein			8.5	4.3	
655	AcrB/AcrD/AcrF multidrug efflux protein		3.2	3	4.1	3.4

Table 2. Continued

Spot ID	Protein name	C3	C8	C13	C24	C30
723	RplB, ribosomal protein L2	6.1	4.8			4.6
725	Pnp, polyribonucleotide nucleotidyltransferase	2.1	4.1			
748	RpsE, ribosomal protein S5			2.4		6.4
827	conserved hypothetical protein		3.2			3.4
888	ribosomal 5S rRNA E-loop binding protein Ctc/L25/TL5	2.7	4.4		11	2
889	ribosomal 5S rRNA E-loop binding protein Ctc/L25/TL5	2.2	6.3			
969	hypothetical transaldolase	2.7	12.3			
970	kinase, hypothetical			4.1	4.4	4.6
1004	RplI, ribosomal protein L9	12.7	18.2	11.4	6.6	
1011	RplI, ribosomal protein L9				2.7	7.5
1078	peptide release factor 2		6.6			2.5
1141	acetyltransferase, GNAT family	2.5	2.2			
1279	Hfq, host factor-I protein	2.3	3.1			
1393	EtfB, electron transfer flavoprotein, beta subunit			2.2	2.8	3.2

abortus, was also decreased in mutants C3 and C8.

Discussion

Brucellosis is a re-emerging zoonosis that can infect not only animals but also humans throughout the world. At present, the pathogenesis of the disease is reported to have greatly increased [19,24]. Despite many studies, however, eradication of brucellosis remains a difficult task, and many potential effective diagnostics and vaccines are under study to prevent the spread of this disease [6,18].

In this study, *B. abortus* mutants were generated by using the EZ-Tn5 transposon system. The resulting mutants were commonly resistant to kanamycin, and the expression of their proteins was different due to the insertion of the related *rKan* gene. The expression patterns of the proteins of the *B. abortus* mutants were generated, compared to *B. abortus* wild-type, and found to vary. We identified various proteins that were changed following transposon insertion and confirmed functions of each protein.

ClpB, shown to increase in expression commonly in *B. abortus* mutants C13, C24, and C30, is associated with energy-related metabolism including ATP-binding and peptidase activity. In addition, ClpB is a heat-shock protein that allows pathogens to adapt to the intracellular environment; moreover, ClpB works in conjunction with DnaK, DnaJ, and GrpE to suppress protein aggregation, thereby affecting pathogenicity [31]. DnaK (Hsp70), which increased in expression in all of the studied *B. abortus* mutants, is a chaperone protein. Protein folding is also performed by DnaK, and ATP is essential for this role. It is also reported that structural change in DnaK occurs through ATPase activity [4]. Moreover, DnaK is involved in replication of phage lambda DNA, is related to hyperosmotic shock, and has a role in ATP-dependent resolubilization of aggregations of protein in conjunction with ClpB. Binding of ClpB occurs according to a previous DnaK association with the protein aggregation. The bi-chaperone network of DnaK and ClpB consists of three stages. When DnaJ is attached, the co-chaperone forms an aggregation with DnaK, and DnaK interacts with ClpB on the surface on the aggregation. The TRP domain protein also has an important role in stimulating the molecular chaperone complex, particularly in the formation of bridges between Hsp70 (DnaK) and Hsp90 [1,2,5,23,31].

RpsC was identified as ribosomal protein S3, which is involved in the expression of the nuclear factor kappa B (NF-κB)-induced reporter gene when T cell stimulation occurs. When the T cell is stimulated, RpsC is transferred into the cell to transmit the NF-κB signal within the cytoplasm. In particular, RpsC has an important role in signal transduction of NF-κB though p65, where NF-κB has an important role in the expressions of genes that bind to regulatory sites or are regulated by p65 [28]. This suggests that not only growth but also T cell stimulation may occur more actively in mutants C24 and C30, which are faster growing than *B. abortus* wild-type.

The SecA, GAPDH, and GNAT family, which are commonly expressed in the mutants C3 and C8 that have slower growth than that in *B. abortus* wild-type. It is thought that the growth rate is lower than that in *B. abortus* wild-type due to expression decreases in metabolic function- related factors active in obtaining the energy required for the normal growth of the strains [9,27]. In addition, the decrease in the expression of AcnA, which is directly related to the growth feature of the strain, in related to regulation networks, such as CRP, ArcA, Fur, and SoxR5, and seems to have affected the growth features of the mutants [12]. Hfq, showing decreased expression in mutants C3 and C8, is an RNA-binding protein that is common

Table 3. Peptide analysis results obtained by liquid chromatography tandem mass spectrometry showing increased and decreased proteins

Spot No.	Gene name	Gene ID	Protein identification	Protein ID	Accession No.	Sequence length	Locus tag	Score	Molecular weight		*pI*	Sequence coverage (%)	Subcellular location	COG functional category
									Experimental	Theoretical				
Increased protein														
32	SoxA	3339477	MULTISPECIES: sarcosine oxidase subunit alpha [Brucella]	WP_002967112.1	WP_002967112	1,344	BruAb1_0226	16	1045.5610	1045.5590	6.29	2	Periplasmic space	E: Glycine cleavage system T protein (aminomethyl-transferase)
102	ClpB	3339973	ATP-dependent Clp protease, ATP-binding subunit ClpB	WP_002964938.1	WP_002964938	2,625	BruAb1_1843	1606	51593.5287	51593.5453	5.18	30	Cytoplasm	O: ATP-dependent protease Clp, ATPase subunit
202	DnaK	3341115	chaperone protein DnaK	WP_002969217.1	AAX75397.1	1,914	BruAb1_2100	503	18108.8404	18108.8666	4.85	16	Cytoplasm	O: Molecular chaperone DnaK (HSP70)
234	BruAb2_0037	3341882	magnesium ion-transporting ATPase, E1-E2 family	WP_002971302.1	AAX75488.1	2,718	BruAb2_0037	17	931.4719	931.4723	6.54	1	Inner membrane	P: Magnesium-transporting ATPase (P type)
369	Zwf	3342337	glucose-6-phosphate 1-dehydrogenase	WP_002965865.1	WP_002965865	1,476	BruAb1_0454	41	844.4477	844.4443	5.74	1	Cytoplasm	G: Gulucos-6-phosphate 1-dehydrogenase
418	DadA	3341955	D-alanine dehydrogenase, small subunit	WP_002965723.1	AAX75742.1	1.251	BruAb2_0309	21	785.4629	785.4647	6.47	1	Cytoplasm	E: Alanine de-hydrogenase
464	BruAb1_1816	3340394	carboxyl-terminal protease	WP_002964915.1	AAX75131.1	1,329	BruAb1_1816	788	23777.4215	23777.4214	5.69	37	Periplasmic space	O: C-terminal processing CtpA/Prc, contains a PDZ domain
483	BruAb2_1038	3341806	hypothetical peptide ABC transporter, permease protein	WP_002965559.1	AAX76414.1	834	BruAb2_1038	25	813.5066	813.5072	10.52	2	Inner membrane	–
572	BruAb1_0662	3339996	hypothetical protein	WP_01168934.1	AAX74037.1	93	BruAb1_0662	21	936.4529	936.4586	11.13	27	Cytoplasm	–

Table 3. Continued

Spot No.	Gene name	Gene ID	Protein identification	Protein ID	Accession No.	Sequence length	Locus tag	Score	Molecular weight		*pI*	Sequence coverage (%)	Subcellular location	COG functional category
									Experimental	Theoretical				
631	BruAb1_1941	3340562	methionine-gamma-lyase, hypothetical	WP_002967006.1	AAX75247.1	1,284	BruAb1_1941	29	801.4242	801.4232	6.02	1	Cytoplasm	–
673	ArgF	3339044	ornithine carbamoyltransferase	WP_002963466.1	AAX73728.1	939	BruAb1_0328	124	2868.4788	2868.4716	5.50	8	Cytoplasm	E: Ornithine carbamoyltransferase
742	BruAb1_0941	3340129	ABC transporter, ATP-binding protein	WP_002964056.1	AAX74305.1	756	BruAb1_0941	76	1145.5879	1145.5928	5.00	3	Cytoplasm	O: Fe-S cluster assembly ATPase SufC
813	TrpA	3340522	tryptophan synthase, alpha subunit	WP_002965172.1	AAX75382.1	840	BruAb1_2083	179	6209.2546	6209.2628	5.48	11	Cytoplasm	E: Tryptophan synthase beta unit
848	RpsC	3341103	ribosomal protein S3	WP_002964356.1	AAX74570.1	711	BruAb1_1232	269	5705.9082	5705.9031	9.86	22	Cytoplasm	J: Ribosomal protein S3
855	RpsC	3341103	ribosomal protein S3	WP_002964356.1	AAX74570.1	711	BruAb1_1231	77	1619.9500	1619.9471	9.86	6	Cytoplasm	J: Ribosomal protein S3
870	RpsC	3341103	ribosomal protein S3	WP_002964356.1	AAX74570.1	711	BruAb1_1231	136	2381.3369	2381.3325	9.86	9	Cytoplasm	J: Ribosomal protein S3
995	AtpH	3341000	ATP synthase F1, delta subunit	WP_002964879.1	AAX75099.1	561	BruAb1_1782	179	6730.6430	6730.6511	8.04	22	Cytoplasm	C: F0F1-type ATP synthase, delta subunit
1034	BruAb1_1108	3339761	single-stranded DNA-binding protein family	WP_002964231.1	AAX74449.1	507	BruAb1_1108	117	3031.6063	3031.6011	5.93	11	Extracellular space	L: Single-stranded DNA-binding protein
1037	RpsE	3340115	ribosomal protein S5	WP_002964345.1	AAX74559.1	561	BruAb1_1221	97	4854.4607	4854.4468	10.49	21	Cytoplasm	J: Ribosomal protein S5
1060	BruAb1_0425	3339291	TPR domain protein	WP_002963560.1	AAX73821.1	1,866	BruAb1_0425	28	1808.8108	1808.8141	6.23	1	Periplasmic space	–
1073	RplM	3339415	ribosomal protein L13	WP_002963926.1	AAX74173.1	465	BruAb1_0805	39	842.5000	842.4974	10.18	5	Cytoplasm	J: Ribosomal protein L13
1118	Dut	3340298	deoxyuridine 5-triphosphate nucleotidohydrolase	WP_002964766.1	AAX74979.1	474	BruAb1_1660	137	3619.1198	3619.1189	6.59	22	Cytoplasm	–

Table 3. Continued

Spot No.	Gene name	Gene ID	Protein identification	Protein ID	Accession No.	Sequence length	Locus tag	Score	Molecular weight		*pI*	Sequence coverage (%)	Subcellular location	COG functional category
									Experimental	Theoretical				
1120	BruAb1_1680	3339640	Outer membrane lipoprotein Omp16	P0A3S9	P0A3S9.1	507	BruAb1_1680	56	960.4848	960.4876	9.92	5	Outer membrane	–
1138	AhpD	3342335	alkyl hydroperoxide reductase D	WP_002965934.1	AAX75942.1	528	BruAb1_0523	154	3690.0771	3690.0777	6.13	16	Cytoplasm	–
1153	BruAb1_1171	3340675	conserved hypothetical protein	WP_002964292.1	AAX74510.1	465	BruAb1_1171	283	5800.9132	5800.9169	5.87	24	Cytoplasm	–
1154	BruAb2_0362	3341616	sugar-phosphate isomerases, RpiB/LacA/LacB family	WP_002965776.1	AAX75793.1	456	BruAb2_0362	413	10359.2240	10359.2292	5.11	50	Cytoplasm	G: Ribose 5-phosphate isomerase RpiB
1210	RplX	3340121	ribosomal protein L24	WP_002964351.1	AAX74565.1	312	BruAb1_1227	29	1302.6821	1302.6779	10.24	11	Cytoplasm	J: Ribosomal protein L24
1294	BruAb1_1486	3339880	cold-shock family protein	WP_002964599.1	AAX74814.1	210	BruAb1_1486	190	5612.8591	5612.8557	6.54	43	Cytoplasm	K: Cold-shock protein, CspA family
1410	RpsB	3340672	ribosomal protein S2	WP_002964289.1	AAX74507.1	771	BruAb1_1168	271	6596.5143	6596.5160	5.86	23	Cytoplasm	J: Ribosomal protein S2
1420	Pgk	3340208	phosphoglycerate kinase	WP_002964816.1	AAX75033.1	1,191	BruAb1_1714	40	1089.5295	1089.5302	5.64	2	Cytoplasm	G: Phosphoglycerate kinase
Decreased proteins														
59	SecA	3340541	preprotein translocase, SecA subunit	WP_002956012.1	AAX7530.1	2,721	BruAb1_1921	260	10834.3236	10834.3256	5.15	8	Cytoplasm	U: Preprotein translocase subunit SecA (ATPase, RNA helicase)
95	AcnA	3340768	aconitate hydratase 1	WP_002965341.1	AAX73506.1	2,688	BruAb1_0090	268	11360.5575	11360.5663	5.55	7	Cytoplasm	–
161	EtfA	3340252	electron transfer flavoprotein, alpha subunit	WP_002965036.1	AAX75250.1	930	BruAb1_1946	44	800.4489	800.4504	4.75	2	Cytoplasm	C: Electron transfer flavoprotein, alpha subunit

Table 3. Continued

Spot No.	Gene name	Gene ID	Protein identification	Protein ID	Accession No.	Sequence length	Locus tag	Score	Molecular weight		*pI*	Sequence coverage (%)	Subcellular location	COG functional category
									Experimental	Theoretical				
216	Nus A	3340636	N utilization substance protein A	WP_002965225.1	AAX75432.1	1,614	BruAb1_2136	108	2793.4055	2793.4004	4.53	4	Cytoplasm	–
299	BruAb1_0708	3339393	cytosol aminopeptidase family protein	WP_002963831.1	AAX74083.1	1,494	BruAb1_0708	41	1415.7213	1415.7144	5.64	2	Cytoplasm	–
322	RplK	3340094	ribosomal protein L11	WP_002964374.1	AAX74590.1	429	BruAb1_1252	14	762.3722	762.3694	9.81	4	Periplasmic space	J: Ribosomal protein L11
342	BruAb1_0708	3339393	cytosol aminopeptidase family protein	WP_002963831.1	AAX74083.1	1,494	BruAb1_0708	23	844.4579	844.4555	5.90	1	Cytoplasm	–
371	Bab_RS30125	23672579	MULTISPECIES: glycerol kinase	WP_002972023.1	KFJ53326.1	1,071	Bab_RS30125	53	833.4765	833.4759	5.18	2	Cytoplasm	C: Glycerol kinase
478	FabB	3340645	3-oxoacyl-(acyl-carrier-protein) synthase I	WP_002965234.1	AAX75440.1	1,224	BruAb1_2145	93	2860.4601	2860.4641	5.21	6	Cytoplasm	IQ: 3-oxoacyl-(acyl-carrier-protein) synthase I
529	Tuf-1	3340098	translation elongation factor Tu	WP_002970090.1	AAX74578.1	1,176	BruAb1_1225	252	7572.7814	7572.7943	5.29	14	Cytoplasm	J: Translation elongation factor EF-Tu, a GTPase
574	BruAb1_0327	3339138	acetylornithine aminotransferase, hypothetical	WP_002963465.1	AAX73727.1	1,212	BruAb1_0327	293	9938.0735	9938.1332	5.63	14	Cytoplasm	–
610	Gap	3340207	glyceraldehyde 3-phosphate dehydrogenase	WP_002964815.1	AAX75032.1	1,008	BruAb1_1713	151	3806.0224	3806.0216	6.00	11	Cytoplasm	G: Glyceraldehyde-3-phosphate dehydrogenase/erythrose-4-phosphate dehydrogenase
612	BruAb2_0572	3341828	renal dipeptidase family protein	WP_002967282.1	AAX75989.1	1,061	BruAb2_0572	112	4278.0898	4278.0940	5.40	10	Cytoplasm	–
648	ilvC	3340151	ketol-acid reductoisomerase	WP_002964491.1	AAX74707.1	1,020	BruAb1_1376	201	7279.8913	7279.8763	5.90	16	Cytoplasm	EH: Ketol-acid reductoisomerase

Table 3. Continued

Spot No.	Gene name	Gene ID	Protein identification	Protein ID	Accession No.	Sequence length	Locus tag	Score	Molecular weight		*pI*	Sequence coverage (%)	Subcellular location	COG functional category
									Experimental	Theoretical				
653	BruAb1_2049	3339680	conserved hypothetical protein	WP_002971854.1	AAX75350.1	696	BruAb1_2049	23	846.4254	846.4269	4.67	3	Cytoplasm	–
655	BruAb1_0303	3339120	multidrug efflux protein	WP_002966673.1	AAX73706.1	3,132	BruAb1_0303	18	930.4541	930.4454	5.00	0	Inner membrane	–
723	RplB	3341106	ribosomal protein L2	WP_002964359.1	AAX74573.1	834	BruAb1_1235	51	6836.2135	6836.2242	10.92	11	Periplasmic space	J: Ribosomal protein L2
725	Pnp	3340642	polyribonucleotide nucleotidyltransferase	WP_002965231.1	AAX75438.1	2,145	BruAb1_2142	26	807.4117	807.4126	5.04	1	Cytoplasm	–
748	RpsE	3340115	ribosomal protein S5	WP_002964345.1	AAX74559.1	561	BruAb1_1221	29	764.4063	764.4068	10.49	3	Cytoplasm	J: Ribosomal protein S5
827	BruAb1_0886	3339354	conserved hypothetical protein	WP_002964004.1	AAX74251.1	708	BruAb1_0886	144	4903.3185	4903.3087	4.98	14	Periplasmic space	–
888	BruAb1_1524	3340810	ribosomal 5S rRNA E-loop binding protein Ctc/L25/TL5	WP_002964640.1	AAX74852.1	624	BruAb1_1524	343	8459.2338	8459.2224	5.91	27	Cytoplasm	–
889	BruAb1_1524	3340810	ribosomal 5S rRNA E-loop binding protein Ctc/L25/TL5	WP_002964640.1	AAX74852.1	624	BruAb1_1524	116	3099.9475	3099.9473	5.91	14	Cytoplasm	–
969	BruAb1_1785	3341003	hypothetical transaldolase	WP_002966970.1	AAX75102.1	654	BruAb1_1785	74	1999.0578	1999.0626	5.47	8	Cytoplasm	–
970	BruAb1_2045	3339676	kinase, hypothetical	WP_002965134.1	AAX75346.1	603	BruAb1_2045	147	11956.3411	11956.3551	6.86	19	Cytoplasm	H: Diphospho-CoA kinase
1004	RplI	3339572	ribosomal protein L9	WP_002963608.1	AAX73869.1	570	BruAb1_0474	72	3081.5451	3081.5434	4.86	10	Cytoplasm	J: Ribosomal protein L9
1011	RplI	3339572	ribosomal protein L9	WP_002963608.1	AAX73869.1	570	BruAb1_0474	186	7071.6953	7071.7018	4.86	22	Cytoplasm	J: Ribosomal protein L9
1078	BruAb1_0927	3339338	peptide release factor 2	WP_002964045.1	AAX74291.1	966	BruAb1_0927	14	1111.5257	1111.5233	5.09	2	Cytoplasm	–

Table 3. Continued

Spot No.	Gene name	Gene ID	Protein identification	Protein ID	Accession No.	Sequence length	Locus tag	Score	Molecular weight		*pI*	Sequence coverage (%)	Subcellular location	COG functional category
									Experimental	Theoretical				
1141	BruAb1_1881	3340244	acetyltransferase, GNAT family	WP_002964973.1	AAX75193.1	459	BruAb1_1881	130	6702.4817	6702.4780	6.22	24	Cytoplasm	R: Predicted acetyltransferase, GNAT superfamily
1279	Hfq	3340039	host factor-I protein	WP_002964239.1	AAX74458.1	237	BruAb1_1117	16	1045.5223	1045.5193	7.93	11	Cytoplasm	T: sRNA-binding regulator protein Hfq
1393	EtfB	3340253	electron transfer flavoprotein, beta subunit	WP_002965037.1	AAX75251.1	747	BruAb1_1947	637	16300.6331	16300.6292	7.77	41	Cytoplasm	C: Electron transfer flavoprotein, alpha and beta subunits

pI, isoelectric point; COG, Clusters of Orthologous Groups.

to bacteria and is important in gene expression control. Hfq acts on pairs of small RNA and mRNA and is involved in translation, transcription, and post-transcription networks. It acts on small RNA to inhibit the translation of the 30S and 50S ribosomal subunits and inhibits degradation of small RNA. In addition, Hfq induces cleavage by ribonuclease E (RNase E) of target mRNA. It is also associated with resistance to environmental stressors such as oxidation, acid, and heat [7,25,26]. It is thought that the observed decrease of Hfq expression may be a cause of the slower growth rate in mutants C3 and C8. Furthermore, transcription in these mutants may cause abnormal expression of several genes.

It is well-known that all the biological processes within living organisms are controlled by the various proteins present within the organism. Protein is not only a basic biological component, but also constituents of enzymes, antibodies, and hormones. In addition, proteins are deeply involved in all cell processes, such as DNA replication, RNA transcription, and protein translation, as well as in determining the function of the organism. Protein analysis of the major pathogenic factors of bacteria is of great importance in research into disease eradication or prevention.

Acknowledgments

This study was supported by MSIP (No. 2014R1A2A2A01007291), KHIDI (HI16C2130), the BK21 PLUS Program for Creative Veterinary Science Research, and the Research Institute for Veterinary Science, Seoul National University, Seoul, Republic of Korea.

Conflict of Interest

The authors declare no conflicts of interest.

References

1. **Acebrón SP, Martín I, del Castillo U, Moro F, Muga A.** DnaK-mediated association of ClpB to protein aggregates. A bichaperone network at the aggregate surface. FEBS Lett 2009, **583**, 2991-2996.
2. **Blatch GL, Lässle M.** The tetratricopeptide repeat: a structural motif mediating protein-protein interactions. Bioessays 1999, **21**, 932-939.
3. **Boschiroli ML, Foulongne V, O'Callaghan D.** Brucellosis: a worldwide zoonosis. Curr Opin Microbiol 2001, **4**, 58-64.
4. **Buchberger A, Theyssen H, Schröder H, McCarty JS, Virgallita G, Milkereit P, Reinstein J, Bukau B.** Nucleotide-induced conformational changes in the ATPase and substrate binding domains of the DnaK chaperone provide evidence for interdomain communication. J Biol Chem 1995, **270**, 16903-16910.
5. **Cellier MF, Teyssier J, Nicolas M, Liautard JP, Marti J, Sri Widada J.** Cloning and characterization of the *Brucella ovis* heat shock protein DnaK functionally expressed in

Escherichia coli. J Bacteriol 1992, **174**, 8036-8042.
6. **Christopher S, Umapathy BL, Ravikumar KL.** Brucellosis: review on the recent trends in pathogenicity and laboratory diagnosis. J Lab Physicians 2010, **2**, 55-60.
7. **Cui M, Wang T, Xu J, Ke Y, Du X, Yuan X, Wang Z, Gong C, Zhuang Y, Lei S, Su X, Wang X, Huang L, Zhong Z, Peng G, Yuan J, Chen Z, Wang Y.** Impact of Hfq on global gene expression and intracellular survival in *Brucella melitensis.* PLoS One 2013, **8**, e71933.
8. **DelVecchio VG, Wagner MA, Eschenbrenner M, Horn TA, Kraycer JA, Estock F, Elzer P, Mujer CV.** *Brucella* proteomes--a review. Vet Microbiol 2002, **90**, 593-603.
9. **Driessen AJ.** SecB, a molecular chaperone with two faces. Trends Microbiol 2001, **9**, 193-196.
10. **Finlay BB, Falkow S.** Common themes in microbial pathogenicity revisited. Microbiol Mol Biol Rev 1997, **61**, 136-169.
11. **Franco MP, Mulder M, Gilman RH, Smits HL.** Human brucellosis. Lancet Infect Dis 2007, **7**, 775-786.
12. **Gruer MJ, Guest JR.** Two genetically-distinct and differentially-regulated aconitases (AcnA and AcnB) in *Escherichia coli.* Microbiology 1994, **140**, 2531-2541.
13. **Guzman-Verri C, Manterola L, Sola-Landa A, Parra A, Cloeckaert A, Garin J, Gorvel JP, Moriyon I, Moreno E, Lopez-Goni I.** The two-component system BvrR/BvrS essential for *Brucella abortus* virulence regulates the expression of outer membrane proteins with counterparts in members of the *Rhizobiaceae.* Proc Natl Acad Sci U S A 2002, **99**, 12375-12380.
14. **Lamontagne J, Béland M, Forest A, Côté-Martin A, Nassif N, Tomaki F, Moriyón I, Moreno E, Paramithiotis E.** Proteomics-based confirmation of protein expression and correction of annotation errors in the *Brucella abortus* genome. BMC Genomics 2010, **11**, 300.
15. **Lee HJ, Cha HJ, Lim JS, Lee SH, Song SY, Kim H, Hancock WS, Yoo JS, Paik YK.** Abundance-ratio-based semiquantitative analysis of site-specific N-linked glycopeptides present in the plasma of hepatocellular carcinoma patients. J Proteome Res 2014, **13**, 2328-2338.
16. **Lee J, Kim KY, Lee J, Paik YK.** Regulation of Dauer formation by *O*-GlcNAcylation in *Caenorhabditis elegans.* J Biol Chem 2010, **285**, 2930-2939.
17. **Lee J, Kim KY, Paik YK.** Alteration in cellular acetylcholine influences dauer formation in *Caenorhabditis elegans.* BMB Rep 2014, **47**, 80-85.
18. **McGiven JA.** New developments in the immunodiagnosis of brucellosis in livestock and wildlife. Rev Sci Tech 2013, **32**, 163-176.
19. **Pappas G.** The changing *Brucella* ecology: novel reservoirs, new threats. Int J Antimicrob Agents 2010, **36** (Suppl 1), S8-11.
20. **Park WB, Im YB, Jung MH, Yoo HS.** Molecular characteristics of *Brucella abortus* mutants generated using EZ-Tn5^{Tm} pMOD^{Tm}-3 transposon system. J Prev Vet Med 2015, **39**, 144-152.
21. **Pizarro-Cerdá J, Méresse S, Parton RG, van der Goot G, Sola-Landa A, Lopez-Goñi I, Moreno E, Gorvel JP.** *Brucella abortus* transits through the autophagic pathway and replicates in the endoplasmic reticulum of nonprofessional phagocytes. Infect Immun 1998, **66**, 5711-5724.
22. **Pomastowski P, Buszewski B.** Two-dimensional gel electrophoresis in the light of new developments. Trends Analyt Chem 2014, **53**, 167-177.
23. **Schlee S, Beinker P, Akhrymuk A, Reinstein J.** A chaperone network for the resolubilization of protein aggregates: direct interaction of ClpB and DnaK. J Mol Biol 2004, **336**, 275-285.
24. **Seleem MN, Boyle SM, Sriranganathan N.** Brucellosis: a re-emerging zoonosis. Vet Microbiol 2010, **140**, 392-398.
25. **Valentin-Hansen P, Eriksen M, Udesen C.** The bacterial Sm-like protein Hfq: a key player in RNA transactions. Mol Microbiol 2004, **51**, 1525-1533.
26. **Vogel J, Luisi BF.** Hfq and its constellation of RNA. Nat Rev Microbiol 2011, **9**, 578-589.
27. **Vrontou E, Economou A.** Structure and function of SecA, the preprotein translocase nanomotor. Biochim Biophys Acta 2004, **1694**, 67-80.
28. **Wan F, Anderson DE, Barnitz RA, Snow A, Bidere N, Zheng L, Hegde V, Lam LT, Staudt LM, Levens D, Deutsch WA, Lenardo MJ.** Ribosomal protein S3: a KH domain subunit in NF-kappaB complexes that mediates selective gene regulation. Cell 2007, **131**, 927-939.
29. **Weldingh K, Rosenkrands I, Jacobsen S, Rasmussen PB, Elhay MJ, Andersen P.** Two-dimensional electrophoresis for analysis of *Mycobacterium tuberculosis* culture filtrate and purification and characterization of six novel proteins. Infect Immun 1998, **66**, 3492-3500.
30. **Woods ML 2nd, Bonfiglioli R, McGee ZA, Georgopoulos C.** Synthesis of a select group of proteins by *Neisseria gonorrhoeae* in response to thermal stress. Infect Immun 1990, **58**, 719-725.
31. **Zolkiewski M.** ClpB cooperates with DnaK, DnaJ, and GrpE in suppressing protein aggregation. A novel multi-chaperone system from *Escherichia coli.* J Biol Chem 1999, **274**, 28083-28086.